Autopsy on Active Distribution Networks: A Data-Driven Fault Analysis Using Micro-PMU Data

Alireza Shahsavari[†], Mohammad Farajollahi[†], Emma Stewart[‡], Ciaran Roberts[♯],
Fady Megala[§], Lilliana Alvarez[§], Ed Cortez[§], and Hamed Mohsenian-Rad[†]
[†]Department of Electrical and Computer Engineering, University of California, Riverside, CA, USA
[‡]Global Security, Lawrence Livermore National Laboratory, Livermore, CA, USA
[♯]Grid Integration Group, Lawrence Berkeley National Laboratory, Berkeley, CA, USA
[§]Energy Delivery Engineering, Riverside Public Utilities, Riverside, CA, USA

***Abstract*—In this paper, we conduct a data-driven experimental analysis on a single-phase-to-neutral fault at a distribution grid in Riverside, CA using data from five distribution level phasor measurement units, a.k.a, Micro-PMUs. Of particular interest is to extract the time-line during the fault. With the high resolution, precision, and time synchronization of the data from Micro-PMUs, the hypothesis about optimal operation of protection devices during each period of the fault time-line is examined, followed by exploring the success of coordination between lateral fuse and main feeder recloser. Also, this paper studies the transient effect of fault on the load-level as well as feeder-level. In addition, the response of inverter based resources to fault, specifically to islanding, is observed and the miscoordination between anti-islanding protection of PV inverters and the feeder recloser is deduced. Finally, the effect of the fault on outlying area feeder-level and customer-level is investigated. This paper takes a first step in using micro-PMU data to conducting a detailed analysis, an autopsy, of how different voltage levels are affected by fault switching events in distribution systems.**

***Keywords*: Data-driven analysis, fault analysis, active distribution network, solar generation, synchrophasor data, micro-PMU.**

I. Introduction

Most service interruptions and power quality issues are nowadays initiated due to some sort of fault at distribution grid. Of course, it is impossible in practice to entirely prevent such faults, in particular, those that occur by natural causes or physical accidents. Therefore, utilities must be prepared to rather mitigate the fault impact. This can be done by first crystallizing weakness points; and then by modifying the control and protection parameters to reduce the impact.

In the context of distribution systems, the faults are generally categorized based on the interruption duration, including permanent faults and momentary faults. Statistically speaking, about 80% of all faults that occur at distribution level are temporary in nature [1]. Recloser deployment is an efficient protection scheme against temporary faults [2]. Commonly, reclosers are expected to operate in coordination with lateral fuses to minimize the number of affected customers.

For example, consider a fault occurrence in downstream of a lateral fuse. On one hand, the recloser is set to trip before the minimum melting time of the fuse. On the other hand, the maximum clearing time of the fuse must be smaller than the last delayed trip of recloser, i.e., the lock-out status. Therefore, if the fault is momentary, then all customers experience a momentary interruption with no blown fuse. If the fault is permanent, then the customers in downstream of the faulted lateral fuse experience permanent interruption while the rest of the customers experience only a momentary interruption.

Several efforts have been conducted in the literature to detect fuse-recloser miscoordination as well as to improve their coordination [3]–[5]. Apart from the level of effectiveness of these various methods, there is still a lack of analysis based on experimental data from real-life fault events in order to check and confirm the optimal operation of protection devices during fault time-line. Such experimental analysis has been traditionally a very difficult task due to the difficulty in cross-examining the extremely fast events that occur at different locations of the distribution system during a fault event.

Examining the effects of fault and protection coordination becomes even a more far-reaching task in *active distribution feeders*, i.e., distribution systems that are connected to distributed energy resources (DERs) and distributed generators (DGs). This is a true real-world challenge. For example, the capacity of the installed solar generation units in the US increased by 28% in one year from 2014 to 2015 [6]. In addition to harvesting power from photovoltaic (PV) farms, there is an increase in the penetration of customer-owned behind-the-meter PV panels in recent years [7], [8].

The response of such high penetration level of PV generation units to momentary and permanent faults is yet to be understood by electric utilities. Moreover, the feeder protection settings must now be coordinated also with PV inverter protection system, which adds yet another degree of complexity to an already complex protection system coordination problem. For instance, transient overvoltage occurs when a behind-the-meter PV generation unit continues to feed into an isolated feeder that is affected by a permanent fault [9].

In [10], effective anti-islanding protection schemes are proposed for PV inverters in faulted feeders. However, the optimal operation of inverter protection schemes is yet to be investigated in practice to check for any potential miscoordination between feeder protection devices and inverter protection system during permanent and momentary interruptions.

This paper proposes a novel data-driven experimental analysis on a single-phase-to-neutral fault to identify the operation of protection devices in fast-time scale. Data from five Micro-

This work was supported in part by National Science Foundation grant ECCS 1462530 and Department of Energy grant EE 0008001. The corresponding author is H. Mohsenian-Rad. E-mail: hamed@ece.ucr.edu.

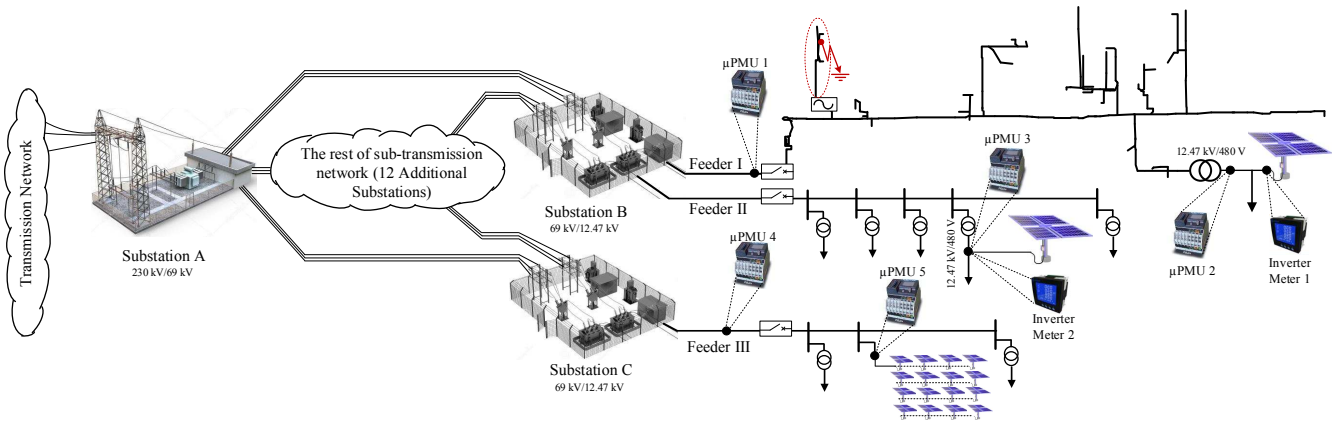

Fig. 1. Test system is a real-life feeder in Riverside, CA, which is equipped with five Micro-PMUs. The fault occurs on Feeder I.

PMUs on a real-life distribution and sub-transmission network is analyzed with the focus on an animal-caused fault on one feeder. We aim to identify the *fault time-line* using feeder-level as well as customer-level Micro-PMUs. In this regard, any potential fuse-recloser miscoordination could be detected using experimental data. In addition, the under-study network includes several PV resources. Thus, the response of the PV resources to the fault is also investigated to explore any mis-coordination between feeder protection scheme and inverter protection systems, i.e., its built-in anti-islanding schemes. Finally, we investigate the effect of the fault on outlying areas covering feeder-level and customer-level impacts.

II. Problem Statement

This study investigates the impact of faults on a power distribution system, in steady state as well as transient conditions, utilizing a real-life distribution network in Riverside, CA. The analysis is based on true measurements and verified field information from utility reports and crew interviews.

The single line diagram of the under-study grid is shown in Fig. 1. The network is operated by Riverside Public Utilities (RPU) [11]. The point of common coupling between the transmission system and the under-study sub-transmission and distribution network is marked as *Substation A*, see Fig. 1. In total, the under-study sub-transmission network includes 15 substations, 69 kV and 33 kV. Of interest in this paper is *Substation B* and to a lesser extend *Substation C*. Two distribution feeders in downstream of Substation B as well as one feeder in downstream of Substation C are included in this study, marked by *Feeders I, II, and III* in Fig. 1.

Feeder I and Feeder II are active distribution feeders, each hosting one 100 kW behind-the-meter PV generation unit, with balanced three-phase inverters. Also, Substation C is interconnected with a 7.5 MW investor-owned behind-the-meter PV farm comprising 25,000 solar panels. The solar generated power is fed into the local distribution grid.

The entire sub-transmission grid of the under-study network is monitored by RPU through a supervisory control and data acquisition (SCADA) system [12]. The default minutely reporting rate of the SCADA system is not sufficient to establish the detailed time-line for the fault event. Fault indicators could be utilized to indicate the presence of a fault, but not the details that are required for evaluating the protection system. The SCADA system could be reconfigured to one reading per-second during a fault, but this additionally would still not be enough to analyze the millisecond nature of the fault events.

Fortunately, RPU is one of few pioneer utilities that has already deployed distribution-level PMUs, a.k.a, Micro-PMUs. The RPU network is equipped with five Micro-PMUs, one at the secondary of a 69 kV to 12.47 kV transformer at Substation B feeding Feeder I, two at the commercial customer locations with the 100 kW PV units at Feeders I and II, one at the secondary of a 69 kV to 12.47 kV transformer at Substation C feeding Feeder III, and one at the point of common coupling of the 7.5 MW PV farm located on Feeder III, see Fig. 1.

Noted that, the last two Micro-PMUs, i.e., Micro-PMU 4 and Micro-PMU 5 are in an outlying area from Micro-PMU 1 and 2, which are close to the fault location of interest. Also, despite Feeders I and II being connected to Substation B, they are *electrically isolated* at this substation. Accordingly, to some extent, we can assume that Micro-PMU 3 too is in an outlying area from Micro-PMU 1 and 2, but it is affected through a different equivalent circuit than Micro-PMUs 4 and 5. In addition to the SCADA system and the installed Micro-PMUs, the two customer-owned behind-the-meter PV panels are monitored by meters with one sample every minute.

The installed Micro-PMUs report four fundamental measurements on three phases, i.e., in total, there are 13 measurement channels: voltage magnitude, voltage phase angle, current magnitude, and current phase angle, with the sampling rate of 120 Hz, i.e., one sample every 8.333 msec. The 13th channel is GPS Lock, utilized to determine if the sensor has established a satellite lock to ensure precise time synchronization. Several studies have recently been conducted by means of Micro-PMU data, see [13]–[17]. As a novel application of Micro-PMU data, we hypothesize that, this high sampling rate, together with direct access to time synchronized voltage and current phasor data at different locations, could allow us study fault event in details within a data-driven framework.

We are interested in answering the following questions with respect to fault events at power distribution systems:

1) What is the time-line of the fault?

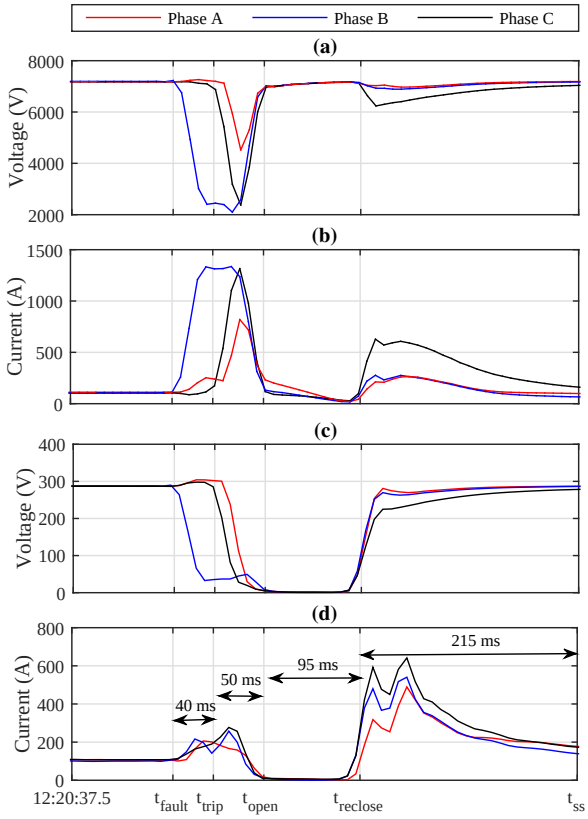

Fig. 2. Three phase voltage magnitude and current magnitude during fault time-line: (a) and (b) Micro-PMU 1, (c) and (d) Micro-PMU 2.

2) Is there any miscoordination between lateral fuses and feeder recloser that is revealed during the fault?
3) What are the effects of fault on PVs and other DERs?
4) Is there any miscoordination between the PV and DER inverter protection system and the main feeder recloser?
5) What is the effect of the fault on outlying resources?

The focus in this paper is the fault occurrence in Feeder I, on a day in November 2016. The fault occurred around noon. The location of the fault is highlighted in Fig. 1, which is close to (almost 0.3 mile away from) Substation B. Utility crews reported that a blown fuse is founded in phase B of the lateral as well as a diseased bird on pole. With the knowledge on the cause for the fault obtained from the outage report, as well as the data collected by Micro-PMUs and inverter meters, the fault event will be studied in details in this paper within a data-driven framework to answer the above questions.

III. Fault Time-Line Analysis

According to the utility outage report, the fault was on phase B and caused by a bird crash. Now, let us look at the recorded voltage and current magnitudes on all phases on Micro-PMU 1 and Micro-PMU 2 that are located at the upstream and the downstream of fault location, as shown in Fig. 2. We can make the following immediate observations from this figure:

1) There exist drastic instantaneous changes in voltage magnitude and current magnitude across *all three phases*. This contradicts our expectation based on the utility outage report that the fault was only on Phase B;

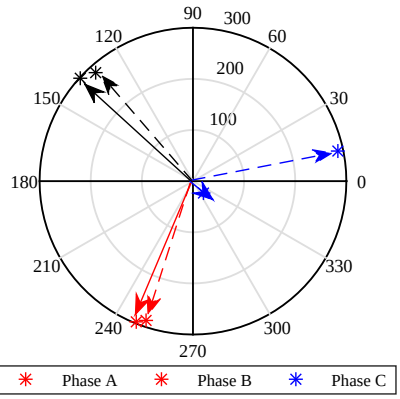

Fig. 3. Three-phase voltage phase angle and magnitude fluctuation of Micro-PMU 2 during fault: dash-line at t_{fault} and solid-line at t_{trip}.

2) The transient in voltage magnitude and current magnitude can be divided into *four perceptible periods*;
3) The changes in voltage and current magnitudes are *not* the same on the upstream versus downstream of the fault.
4) While the voltage magnitude and current magnitude at Micro-PMU 2 drop to zero and stay at zero for almost 95 msec, the voltage magnitude at Micro-PMU 1 almost remains at is nominal level, i.e., around 7200 volts.

Therefore, it is clear that there is more room to investigate beyond what the utility field crew included in their fault report.

Following the second item above, next, we investigate each of the four identified stages that comprise the fault time-line.

A. Stage I

The first stage starts at time t_{fault} and lasts for almost 40 milliseconds, till t_{trip}. During this period, it is assumed that there exists a single phase to neutral fault on phase B, as highlighted in Fig. 1. As it can be seen from Fig. 2, voltage on phase B drops at Substation B by 70%. The amount of such drop depends on fault location and fault resistance. We can see that the deviations in customer voltage on phase B more or less follow those of the substation voltage, see Fig. 2(c). During this period, substation injects fault current on phase B; consequently substation current increases on phase B to almost 1400 A. The hypothesis of a fault existing in phase B is verified by these observations. Note that, fluctuations in current magnitude of Micro-PMU 2 will be studied in the next section with the focus on the effect of fault on PV units.

Another interesting observation during the first stage is the low-magnitude deviation in voltage on phases A and C due to fault occurrence on phase B, see Fig. 3. Based on this figure, the magnitude of voltage on phase B decreases as expected. However, there exist deviations in magnitude of phases A and C, due to changing the neutral of the three-phase system. Note that, the phase-to-neutral fault current with specific fault resistance leads to changing the three-phase neutral.

B. Stage II

At t_{trip}, recloser sends the trip command to the circuit breaker, because the fault current exceeds the recloser instantaneous pick-up current. Thus, it is concluded that during the

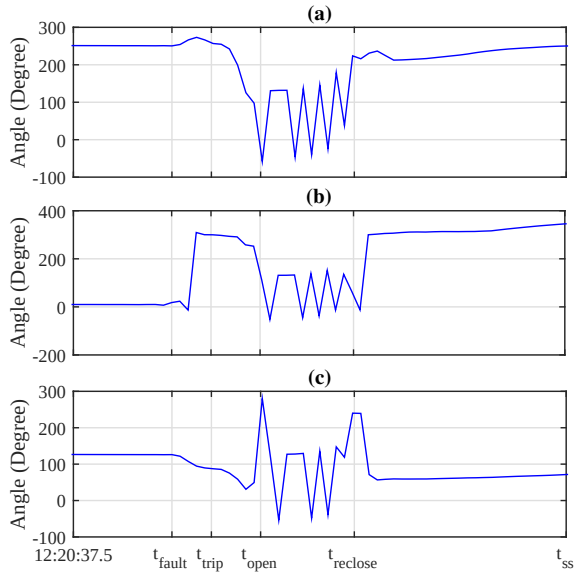

Fig. 4. Current phase angle of Micro-PMU 1 during fault time-line: (a) Phase A (b) Phase B (c) Phase C.

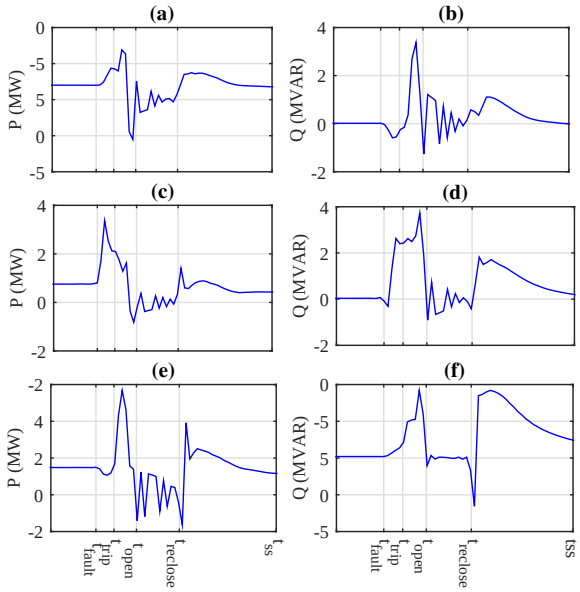

Fig. 5. Active and reactive power at Micro-PMU 1 during fault time-line: (a) and (b) Active and reactive power of phase A (c) and (d) Active and reactive power of phase B (e) and (f) Active and reactive power of phase C.

second stage, the transient is caused by the operation of circuit breaker, which lasts about 50 milliseconds to completely isolate Feeder I from Substation B, at t_{open}. To the extent of our knowledge, the circuit breaker of Feeder I is a three-phase switch, thus all phases are affected during this period.

C. Stage III

During the third stage, Feeder I is isolated from the rest of network. Thus, Micro-PMU 1 reports the grid-side measurements and Micro-PMU 2 reports the measurements on the isolated feeder. As expected, on one hand, the three-phase voltage of Micro-PMU 1 increased to its nominal voltage during this period. On the other hand, the voltage at customer-side drops to zero in this period, since the feeder is isolated by circuit breaker. Also, the customer-side current is zero during this period. All customers in Feeder I must have similarly experienced a momentary outage during this period.

During the third period, the equivalent circuit from Micro-PMU 1 is for the most part the same as an opened RLC circuit. Based on the circuit analysis, when the RLC circuit is opened, its current oscillates around zero with specific damping. As it can be seen from Fig. 2(b), the current of Micro-PMU 1 gradually decreases to zero. Note that the gradual reduction could also be due to the Micro-PMUs internal low pass filters. Also, three-phase current angle in the corresponding period fluctuates about 180 degrees, see Fig. 4. These two observations on the substation current magnitude and the fluctuations in current angle explain the presence of current oscillation in form of the one in an open-circuit RLC circuit. A similar conclusion can be made from the active and reactive power oscillations at substation, as shown in Fig. 5.

D. Stage IV

At t_{reclose}, the first shot of recloser is finished and the feeder is reconnected to substation. The fourth stage starts from t_{reclose} to t_{ss}, where t_{ss} is around the beginning time of the post-fault steady-state. During this period, all loads on this feeder, except for the loads on the downstream of the blown fuse, are *reconnected* to the grid. This causes a disturbance in substation voltage and current magnitudes, see Fig. 2(a) and (b). For instance, the surge current of turning-on the loads in phase C is about six time greater than the pre-fault current. Also, there exists a three-phase surge current in customer-level, i.e., Micro-PMU 2, due to reconnecting the load after reclosing.

Interestingly, but expectedly, some power quality sensitive loads are reconnected with some delay. This issue is better understood by looking at the per-phase steady-state pre-fault and post-fault active and reactive power of Feeder I, which is read by Micro-PMU 1, as in Fig. 6. We can see that, after reclosing, some of the sensitive loads are still disconnected. The reduction in active and reactive power of phase B is more than phase A and C, which verifies that the customers fed by phase B in faulted zone are isolated by blown fuse.

We also examined the coordination between lateral fuses and feeder recloser to detect any possible miscoordination. In practice, the recloser in instantaneous mode must recognize momentary faults, and operate faster than lateral fuses [5]. This clearly was the case in this real-world fault event. However, as we will discuss in Section IV, there might be a fuserecloser miscoordination caused by the additional fault current supplied by DERs in active networks. In general, the coordination between recloser and lateral fuse in active feeders depends on fault type, fault location, generation level of DER, etc.

IV. Responses of PV Resources to Fault

This section aims to study the impact of fault occurrence on grid connected PV generation. The faulted feeder, i.e., Feeder I, includes 100 kW behind-the-meter PV generation.

There was no reverse power flow from PV bus back to the feeder before the fault occurrence. The dash-lines in Fig. 7

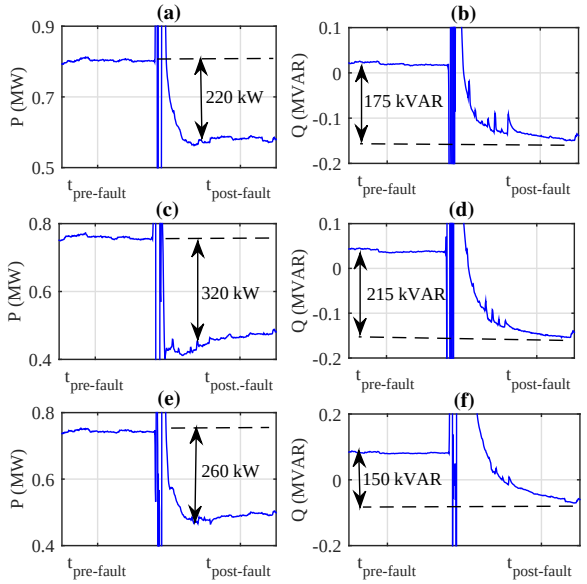

Fig. 6. Active and reactive power at Micro-PMU 1 during fault time-line: (a) and (b) Active and reactive power of phase A (c) and (d) Active and reactive power of phase B (e) and (f) Active and reactive power of phase C.

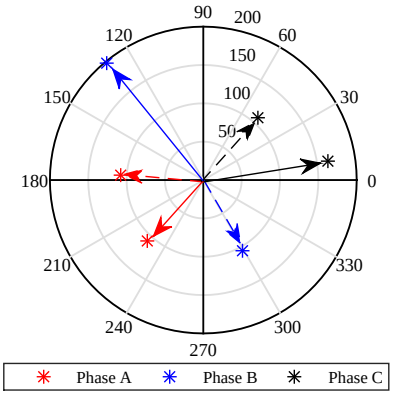

Fig. 7. Three-phase current phase angle and magnitude fluctuation of Micro-PMU 2 during fault: dash-line at t_{fault} and solid-line at t_{trip}.

show the three-phase current magnitude and angle of Micro-PMU 2 at t_{fault}. Before the fault occurrence, the PV bus loads are served partially by the PV unit, and the rest by the main grid. After fault occurrence, however, the current of phase B rotates approximately 180 degrees, and increases in magnitude, see the solid-line in Fig. 7, which means that during Stage I of the fault, the current phase angle reverses its polarity. Based on the current magnitude and phase angle, we can conclude that after fault occurrence, phase B of the PV generation injects power to the fault location. However, Phase A and C of PV generation still injects power to the nearby loads with low-deviation in magnitude and phase.

In practice, almost all grid-tied inverters have a built-in anti-islanding protection scheme to stop feeding power back to the grid during interruption on the side of the feeder. Accordingly, at t_{open} the anti-islanding protection system of PV inverter detects feeder isolation due to recloser tripping, and disconnects itself from the feeder. This hypothesis is justified in Fig. 8. Based on this figure, at $t_{\text{pre-fault}}$ the PV derives 8.11 kW, 9.21 kW, and 5.31 kW from the grid and the rest of power

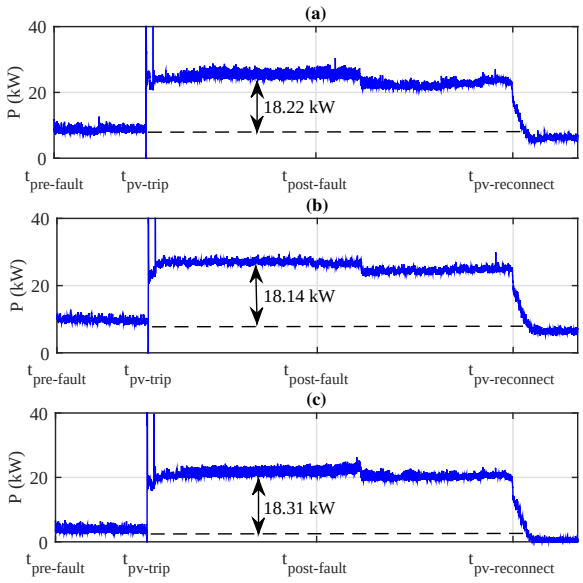

Fig. 8. Active power at Micro-PMU 2 from pre-fault to post-fault: (a) phase A (b) phase B (c) phase C.

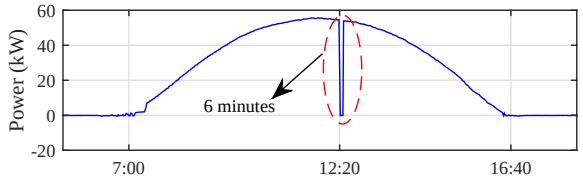

Fig. 9. Active power of PV panel in Feeeder I measured by Inverter Meter 1 including the fault and reclosing time at 12:20.

is supported by PV panels. Whereas, after fault occurrence and recloser operation, the PV panel is still disconnected and the entire loads should be grid fed. According, the active power measured by Micro-PMU 2 increases. After almost 6 minuets, the PV generation is reconnected to the grid and the active power measured by Micro-PMU 2 decreases to pre-fault value, see Fig. 8. This observation also can be made from Invert Meter 1, where the output power of PV drops to zero at 12:20 PM and lasts for about 6 minutes, as shown and marked by ellipse in Fig. 9. Based on this observation, there exists a miscoordination between anti-islanding protection scheme of inverter and feeder recloser. Despite the permanent fault, the PV bus experiences a momentary fault and after $t_{reclosing}$, the fault is cleared by the blown lateral fuse.

Also, the fault causes unusual disturbances on outlying PV units, located on Feeder II and III. However, based on the data of Micro-PMU 3 and 5 as well as Inverter Meter 2 (not shown here), there was no interruption in PV generation output.

V. Fault Effect on Outlying Area

This section briefly investigates the effect of fault on outlying areas, at both customer-level and feeder-level. As mentioned before, though Feeder I and II are fed from the same substation, they are electrically isolated in substation. Therefore, we can treat the data from Micro-PMU 3 as customer-level measurements in an outlying area. Furthermore, there are also two micro-PMUs, i.e., Micro-PMU 4 and 5, that are physically located tens of miles away from the

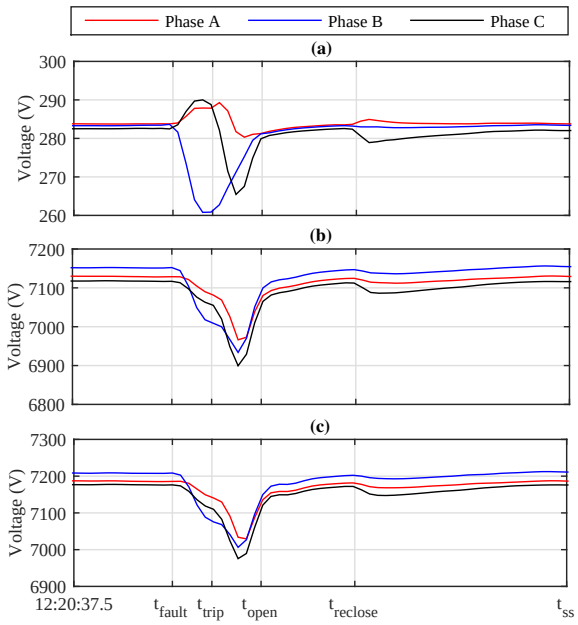

Fig. 10. Synchronized voltage magnitude measurements during fault in three outlying locations: (a) Micro-PMU 3, (b) Micro-PMU 4, (c) Micro PMU 5.

faulted feeder. They too report the effect of fault in additional outlying areas. The three-phase voltage magnitude of these three outlying Micro-PMUs are depicted in Fig. 10.

Based on Fig. 10(a), the fluctuation in voltage magnitude of Micro-PMU 3 during the first stage of the event is similar to the fluctuations observed by Micro-PMUs 1 and 2, see Fig. 2(a) and (c). The reason behind this observation is that the fault affects the voltage of common point of Micro-PMU 2 and 3. Thus Micro-PMU 3 follows the same voltage signature from the common point, of course, with lower-deviation from nominal voltage compared to Micro-PMUs 1 and 2.

From Figs. 10(a) and (b), the voltage magnitude deviations in Micro-PMUs 4 and 5 have different signatures compared to those of Micro-PMUs 1, 2, and 3. The accurate justification for these differences would require additional detailed information on the rest of the system, including the exact grid topology, the type and locations of phase shifters, transformer windings, and voltage regulators between Feeder I and III.

VI. Conclusions and Future Work

A data-driven experimental fault analysis is presented to identify fault time-line in fast-time scales at a real-life distribution and sub-transmission system in Riverside, CA, based on synchronized measurements from five Micro-PMUs. First, the exact time-line of the fault is extracted, followed by discussions on each stage of the time-line. Second, the optimal operation of protective devices during each stage of the time-line is examined. Of particular interest was to investigate the fuse-recloser coordination based on the experimental data from real-life system. Third, the transient response of PV resources to fault, specially during islanding mode, was studied. Our analysis showed a miscoordination between recloser and anti-islanding protection system of the PV unit. Finally, the effect of fault on outlying areas was investigated. It was observed that the outlying areas experienced major power-quality disturbance; the transient of deviations depends on grid parameters.

The results in this paper can be extended in several directions. First, the methodology that is used in this analysis can be repeated to other fault events on the understudy distribution and sub-transmission system. This will allow creating a database for similar autopsy results for a variety of fault occurrences. Second, while the methodology that is used in this paper is mostly intuitive and manual; in future, one can extend the analysis to perform similar data extractions, such as in terms of identifying the different stages of the fault, in an automated fashion using proper algorithms.

References

[1] S. Brahma and A. Girgis, "Development of adaptive protection scheme for distribution systems with high penetration of distributed generation," *IEEE Trans. on power delivery*, vol. 19, no. 1, pp. 56–63, 2004.

[2] M. E. Raoufat, A. Taalimi, K. Tomsovic, and R. Hay, "Event analysis of pulse-reclosers in distribution systems through sparse representation," *Proc. of International Conference on Intelligent System Application to Power Systems*, Sep. 2017.

[3] M.-H. Kim, S.-H. Lim, and J.-C. Kim, "Improvement of recloser-fuse operations and coordination in a power distribution system with SFCL," *IEEE Trans. on Applied Superconductivity*, vol. 21, no. 3, pp. 2209–2212, 2011.

[4] S. Chaitusaney and A. Yokoyama, "Prevention of reliability degradation from recloser–fuse miscoordination due to distributed generation," *IEEE Transactions on Power Delivery*, vol. 23, no. 4, pp. 2545–2554, 2008.

[5] P. H. Shah and B. R. Bhalja, "New adaptive digital relaying scheme to tackle recloser-fuse miscoordination during distributed generation interconnections," *IET Generation, Transmission & Distribution*, vol. 8, no. 4, pp. 682–688, 2014.

[6] S. Akhlaghi, "Efficient operation of residential solar panels with determination of the optimal tilt angle and optimal intervals based on forecasting model," *IET Renewable Power Generation*, April 2017.

[7] H. Moradi, A. Abtahi, and R. Messenger, "Annual performance comparison between tracking and fixed photovoltaic arrays," in *Proc. of the Photovoltaic Specialists Conference (PVSC)*, 2016, pp. 3179–3183.

[8] E. Reihani, M. Motalleb, R. Ghorbani, and L. S. Saoud, "Load peak shaving and power smoothing of a distribution grid with high renewable energy penetration," *Renewable Energy*, vol. 86, pp. 1372–1379, 2016.

[9] A. Eshraghi and R. Ghorbani, "Islanding detection and over voltage mitigation using controllable loads," *Sustainable Energy, Grids and Networks*, vol. 6, pp. 125–135, 2016.

[10] M. Liserre, A. Pigazo, A. Dell'Aquila, and V. M. Moreno, "An anti-islanding method for single-phase inverters based on a grid voltage sensorless control," *IEEE Trans. on Industrial Electronics*, vol. 53, no. 5, pp. 1418–1426, 2006.

[11] [Online]. Available: http://www.riversideca.gov/utilities/

[12] Z. Taylor, H. A.-Hejazi, E. Cortez, L. Alvarez, S. Ula, M. Barth, and H. Mohsenian-Rad, "Battery-assisted distribution feeder peak load reduction: Stochastic optimization and utility-scale implementation," in *Proc. of IEEE PES General Meeting*, Boston, MA, Jul. 2016.

[13] A. Shahsavari, A. Sadeghi-Mobarakeh, E. Stewart, and H. Mohsenian-Rad, "Distribution grid reliability analysis considering regulation down load resources via micro-pmu data," in *IEEE International Conference on Smart Grid Communications*, Sydney, Australia, Nov. 2016.

[14] A. Shahsavari, A. Sadeghi-Mobarakeh, E. Stewart, E. Cortez, L. Alvarez, F. Megala, and H. Mohsenian-Rad, "Distribution grid reliability versus regulation market efficiency: An analysis based on micro-pmu data," *IEEE Trans. on Smart Grid (accepted)*, pp. 1–9, 2017.

[15] A. Shahsavari, M. Farajollahi, E. Stewart, A. von Meier, L. Alvarez, E. Cortez, and H. Mohsenian-Rad, "A data-driven analysis of capacitor bank operation at a distribution feeder using micro-pmu data," in *IEEE PES ISGT*, Washington D.C., Apr. 2017.

[16] M. Farajollahi, A. Shahsavari, and H. Mohsenian-Rad, "Location identification of high impedance faults using synchronized harmonic phasors," in *IEEE PES ISGT*, Washington D.C., Apr. 2017.

[17] M. Jamei, A. Scaglione, C. Roberts, A. McEachern, E. Stewart, S. Peisert, and C. McParland, "Online thevenin parameter tracking using synchrophasor data," in *Proc. of the IEEE PES General Meeting*, Chicago, IL, Jul. 2017.